

Supporting Information

Experiment

Preparation of the cells

Processing of the FTO substrate: The FTO was cut into the desired size, ultrasonically washed with a substrate cleaning fluid for 20 min, soaked overnight in isopropanol solution with the KOH mass fraction of 17%, and after rinsing with deionized water, ultrasonically washed again for 20 min with acetone and ethanol.

Preparation of the dense layer: The FTO after UV ozone treatment for 45 min was treated with an acidic ethanol solution containing tetrabutyl titanate by spin-coating at 2000 rpm for 45 s, followed by sintering at 500 °C for 30 min.

Preparation of the $\text{CH}_3\text{NH}_3\text{PbI}_{3-x}\text{Cl}_x$ perovskite layer: The perovskite precursor solution ($\text{PbCl}_2:\text{CH}_3\text{NH}_3\text{I} = 3:1$; a DMF solution with the mass fraction of 40%) was dropped onto the FTO surface with the prepared compact layer. After spin-coating at 2000 rpm for 30 s, the solution was placed on a hot stage at 100 °C for 60 min, with all operations under the protection of nitrogen.

Preparation of the $\text{CH}_3\text{NH}_3\text{PbI}_{3-x}(\text{SCN})_x$ perovskite layer: The perovskite precursor solution ($\text{Pb}(\text{SCN})_2:\text{PbCl}_2:\text{CH}_3\text{NH}_3\text{I} = x:(3-x):1$; a DMF solution with a mass fraction of 40%) was added to the FTO surface with the prepared compact layer. After spin-coating at 2000 rpm for 30 s, the solution was placed on a hot stage at 100 °C for 60 min, with all operations under the protection of nitrogen.

Preparation of the hole-transport layer: The Spiro-OMeTAD chlorobenzene solution was dropped onto the cell surface and treated for 60 s by spin-coating at 2000 rpm.

Preparation of the counter electrodes: The semitransparent Ag counter electrodes with a magnetron-sputtered thickness of 9 nm were used. No etching process of the FTO substrates is evolved in the fabrication process. The area of the cells is controlled by the size of the mask during the sputtering of the counter electrodes.

Performance of perovskite composite films and device characterization

The photovoltaic performance of the cells was measured in ambient conditions with a Keithley Model 2000 instrument under simulated AM 1.5 sunlight generated by a YSS-5A system (Yamashita DENSO, Japan). The light intensity of the system was calibrated with a standard silicon solar cell, and its active area was fixed at 0.0314 cm². EQE measurements were performed with a solar cell monochromatic

incident photon-to-electron conversion efficiency measurement system (SCS10-X150-DSSC, Zolix); the active area of the test samples was 6 mm². Film morphology and EDS mapping of the perovskite layer were observed by field-emission SEM (S-4800 Hitachi, Japan). Photoshop 2015.5 software was used to process the SEM images of perovskite layer from different precursor ratio to calculate to perovskite coverage. The coverage of the layer is in accordance with ratio of the pixel statistics of the active layer to the picture pixel. The crystal structures of the composite perovskite films were investigated with an X-ray diffractometer (D/MAX-PC 2500, Rigaku).

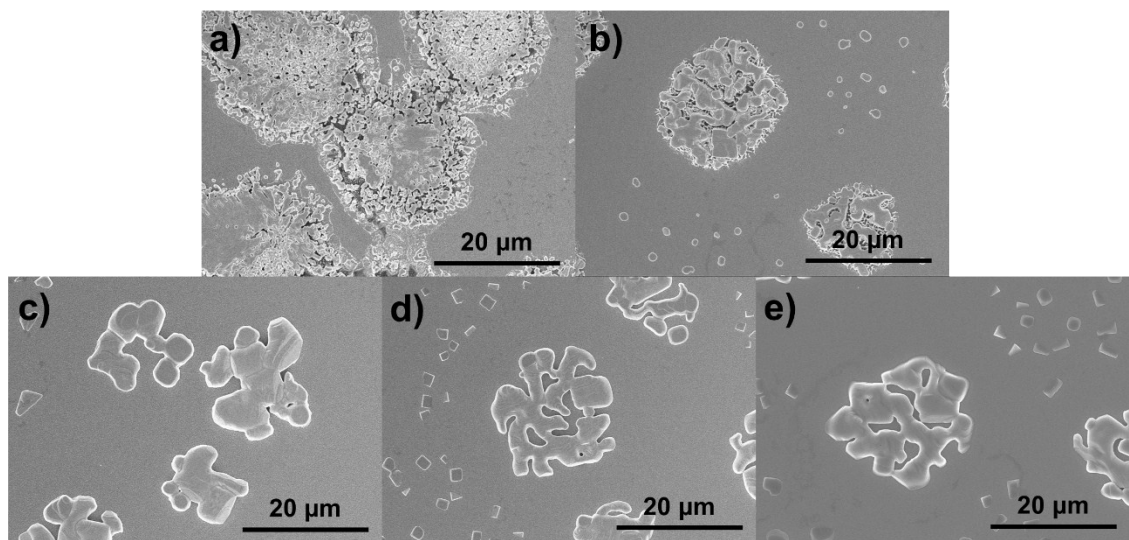


Fig. S1 SEM of the Perovskite Precursor Film After the Annealing at 100 °C for (a) 0 min, (b) 2 min, (c) 5 min, (d) 30 min, and (e) 60 min

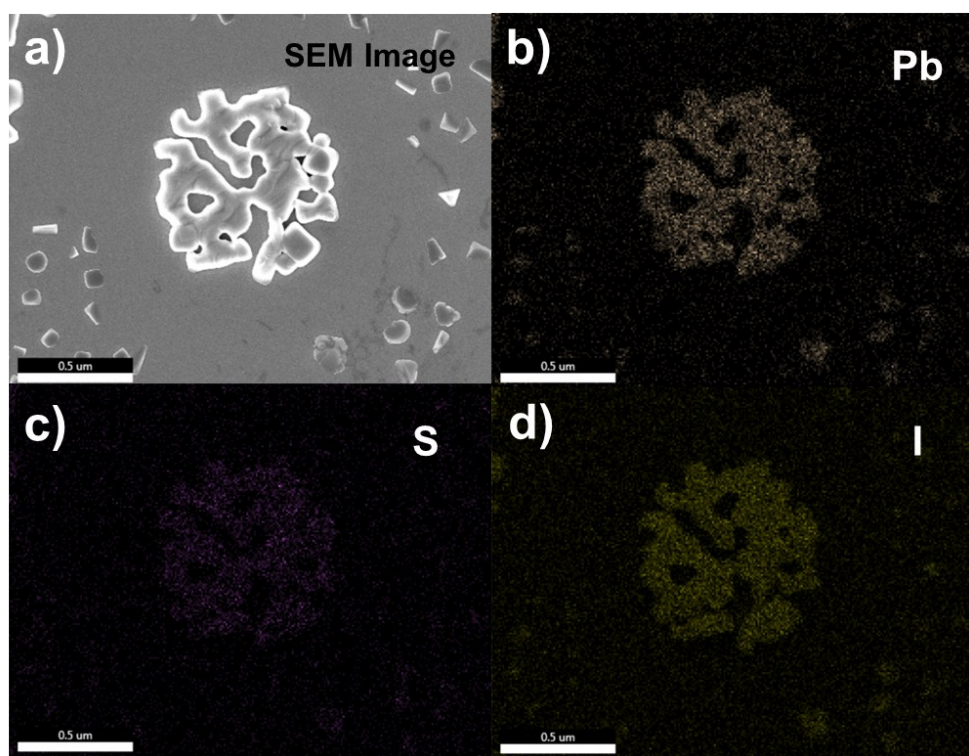


Fig. S2 (a) SEM of the $\text{CH}_3\text{NH}_3\text{PbI}_{3-x}(\text{SCN})_x$ Island-like Structures and (b–d) Photoelectron Spectroscopy of the Distribution of Elemental (b) Pb, (c) S, and (d) I

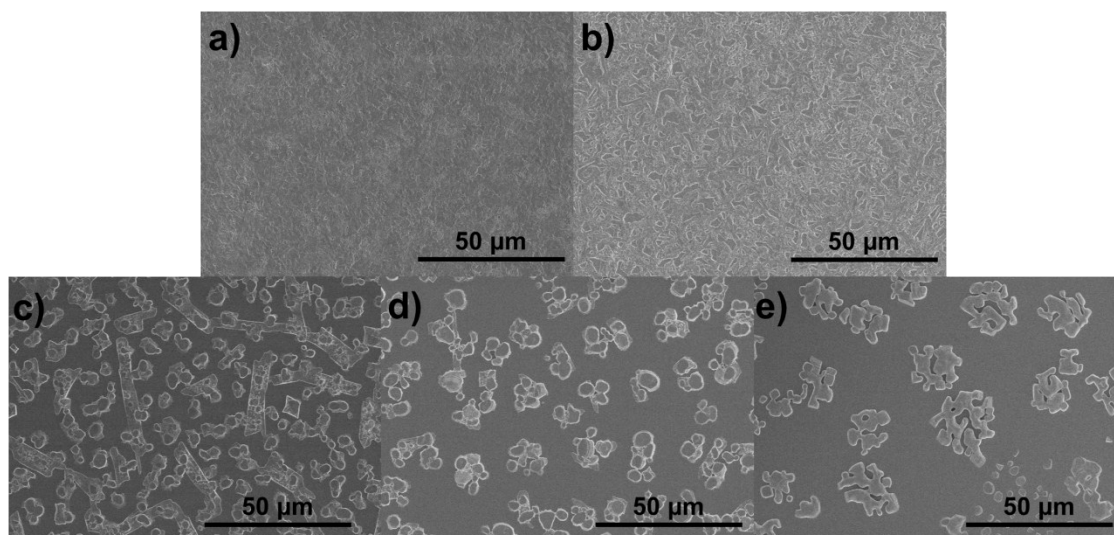


Fig. S3 SEM of Perovskite Films Prepared with the Precursor Solution and Different $\text{Pb}(\text{SCN})_2$ Content; proportion of $\text{Pb}(\text{SCN})_2$, PbCl_2 , and $\text{CH}_3\text{NH}_3\text{I}$ in the precursor solution is $x:(1-x):3$ with (a) $x = 0$, (b) $x = 0.25$, (c) $x = 0.5$, (d) $x = 0.75$, and (e) $x = 1$

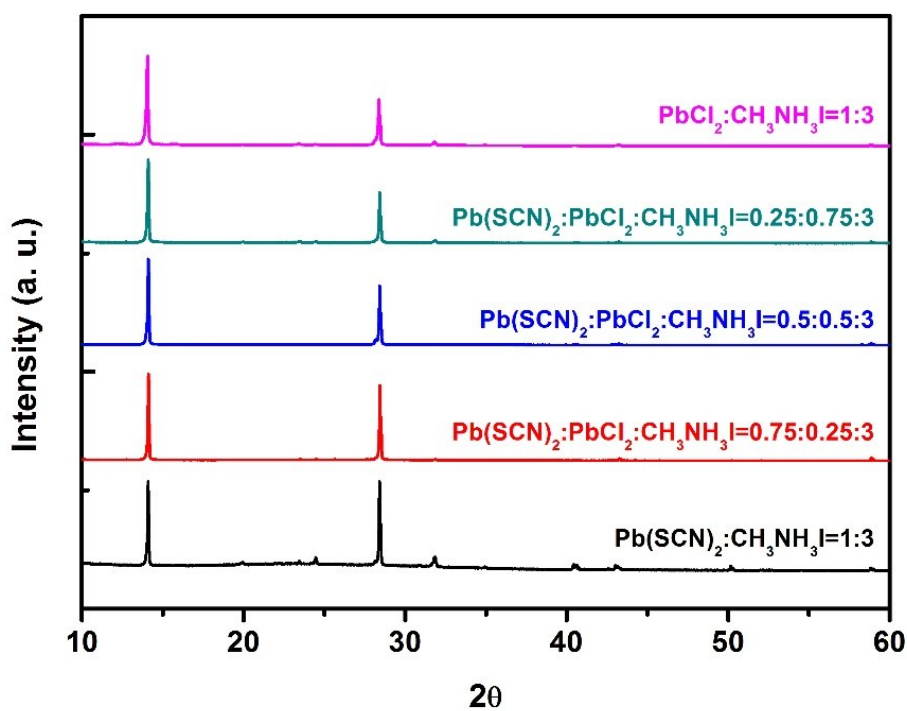


Fig. S4 XRD Spectra of Perovskite Films Prepared with the Precursor Solution and Different $\text{Pb}(\text{SCN})_2$ Content, proportion of $\text{Pb}(\text{SCN})_2$, PbCl_2 , and $\text{CH}_3\text{NH}_3\text{I}$ in the precursor solution is $x:(1-x):3$ with (a) $x = 0$, (b) $x = 0.25$, (c) $x = 0.5$, (d) $x = 0.75$, and (e) $x = 1$

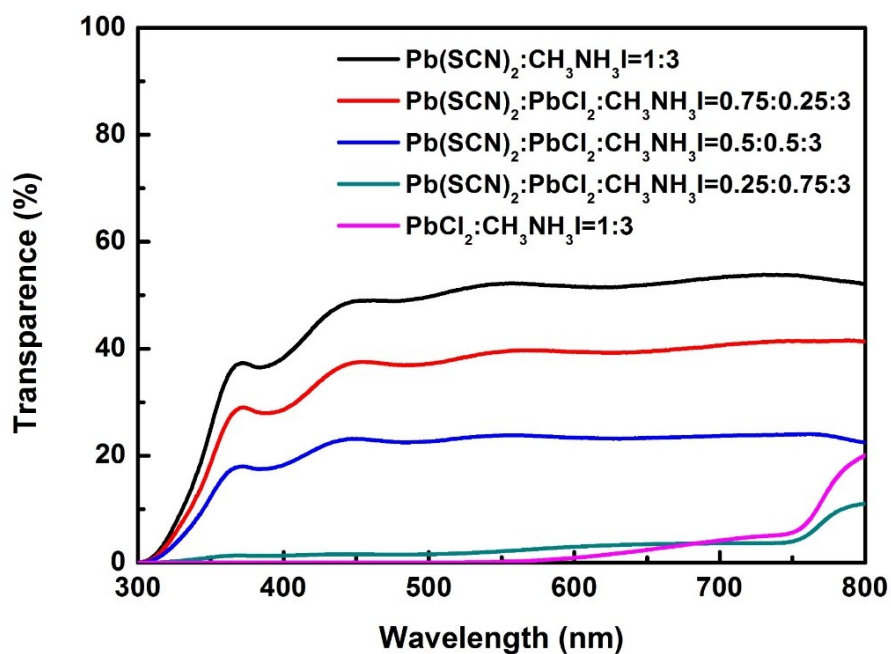


Fig. S5 Transmittance Spectra of devices (FTO/t-TiO₂/perovskite/Spiro) Prepared with the Precursor Solution and Different Pb(SCN)₂ Content

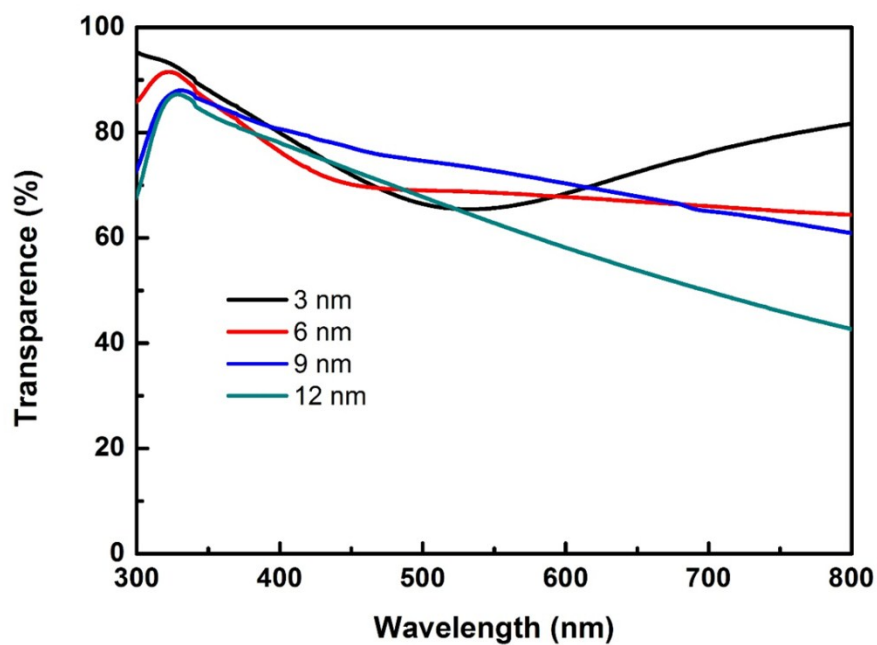


Fig. S6 Transmittance of Ag Electrodes with Different Thicknesses

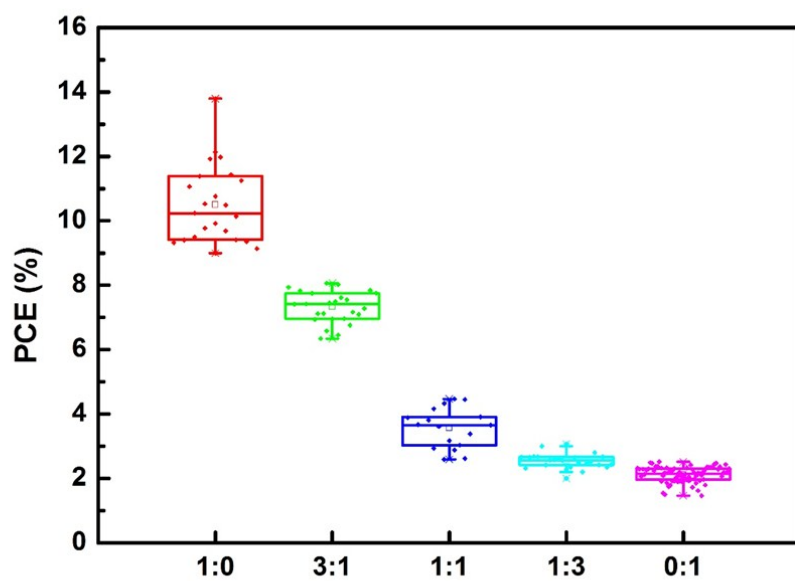


Fig. S7 Efficiency Distribution of Perovskite Solar Cells Prepared with the Precursor Solution and Different Pb(SCN)₂ Content

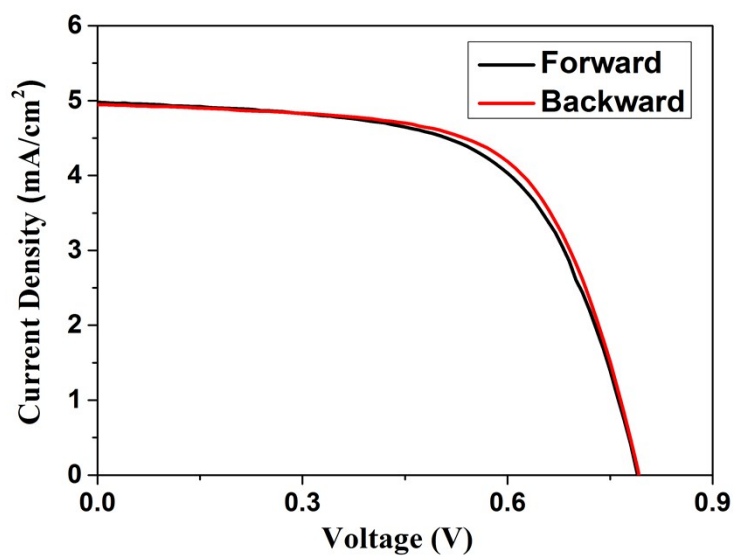


Fig. S8 J–V Curves for Hysteresis Tests of device (prepared from precursor solution of $\text{Pb}(\text{SCN})_2 : \text{CH}_3\text{NH}_3\text{I}=1:3$) under AM1.5G Illumination

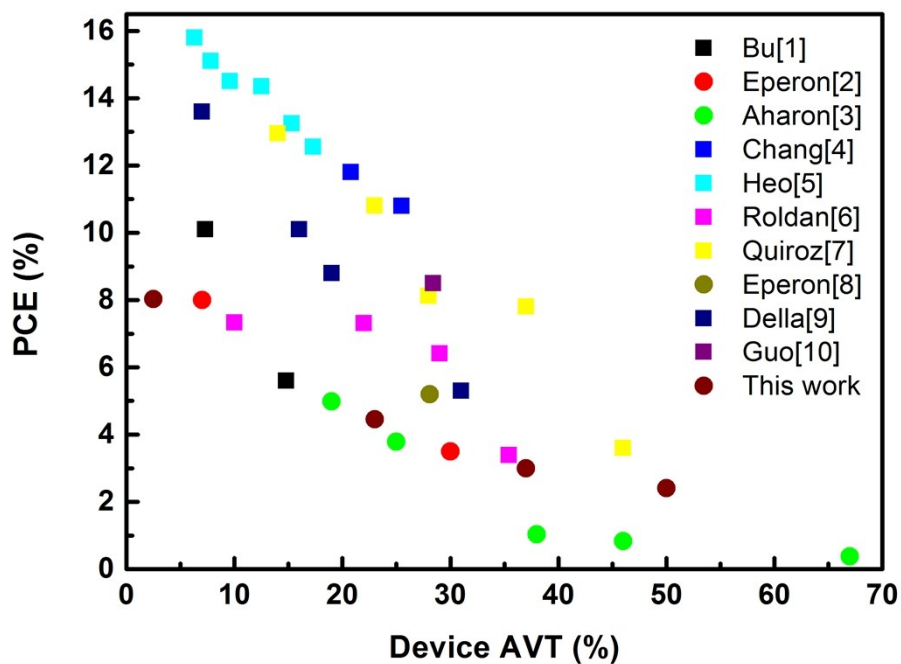


Fig. S9 Comparison of Perovskite Solar Cells from the Present Work with Other Previously Reported Semitransparent Perovskite Solar Cells in Terms of Performance

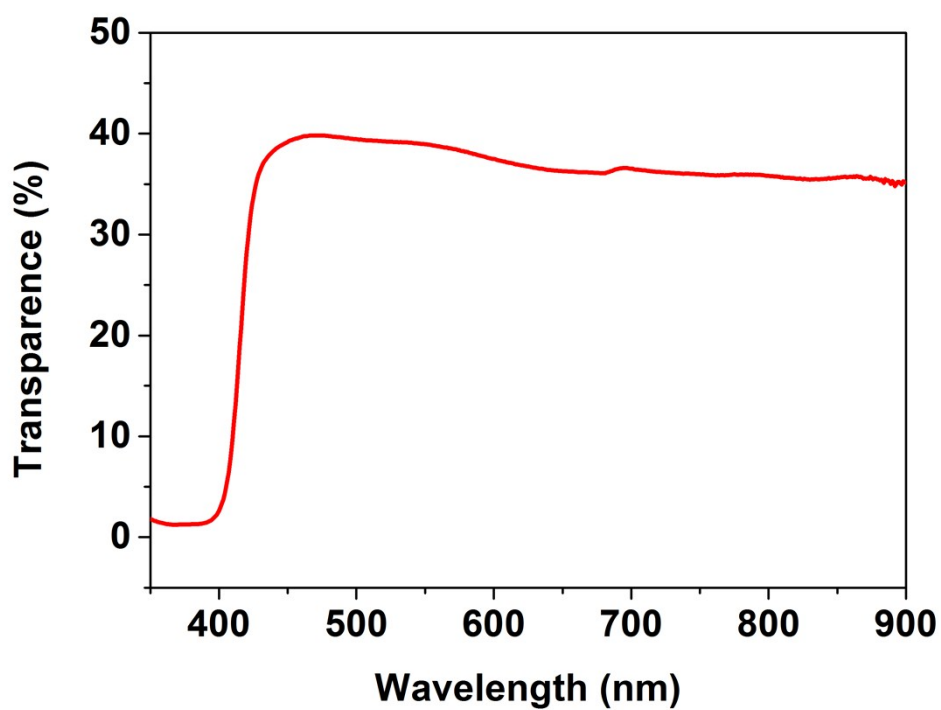
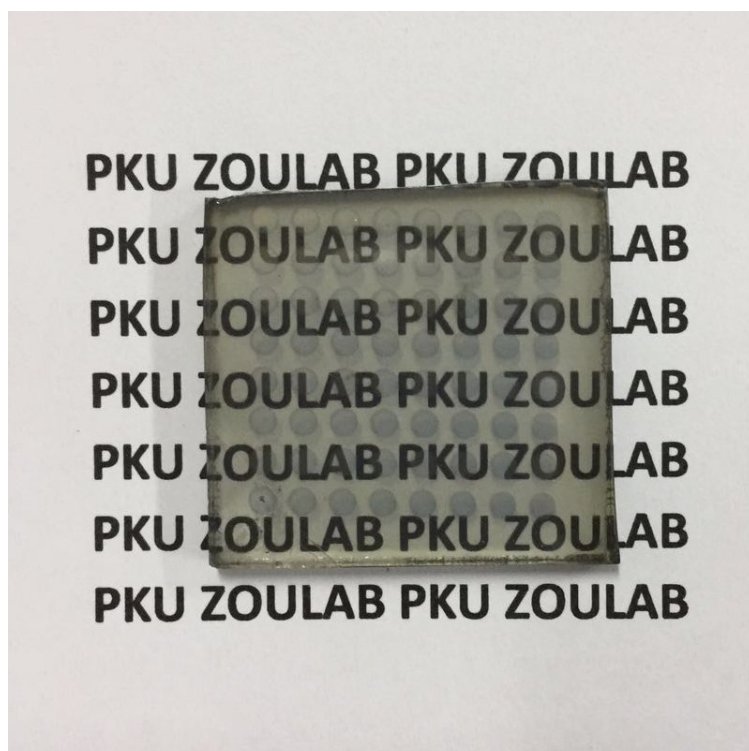


Fig.S10 The Transmittance Spectra as well as Optical Photograph of Full Solar Cell Devices(prepared from precursor solution of $\text{Pb}(\text{SCN})_2 : \text{CH}_3\text{NH}_3\text{I}=1:3$).

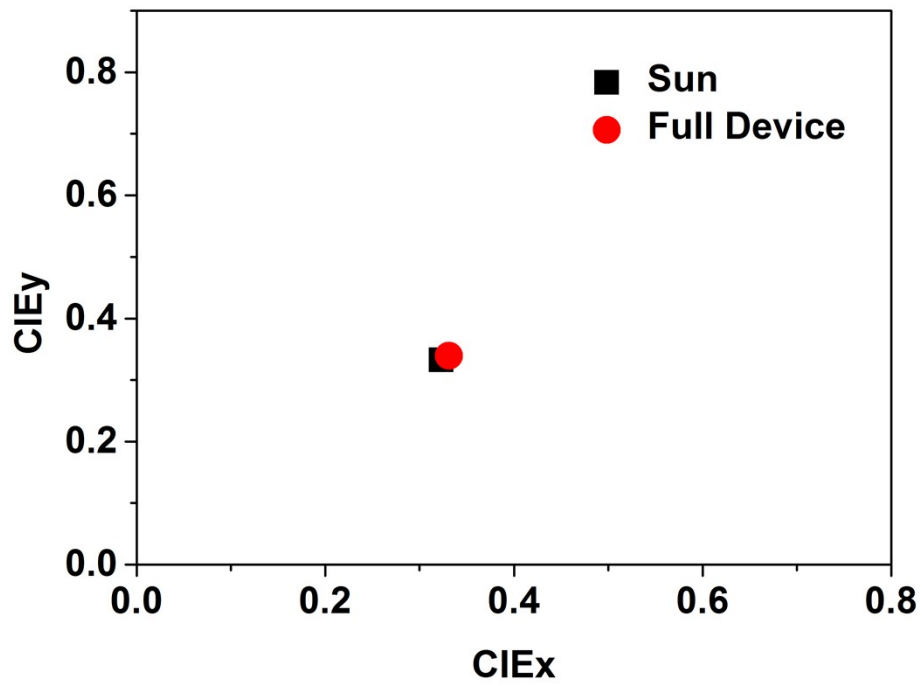


Fig.S11 Color Coordinates of Full Solar Cell Devices (prepared from precursor solution $\text{Pb}(\text{SCN})_2 : \text{CH}_3\text{NH}_3\text{I}=1:3$)

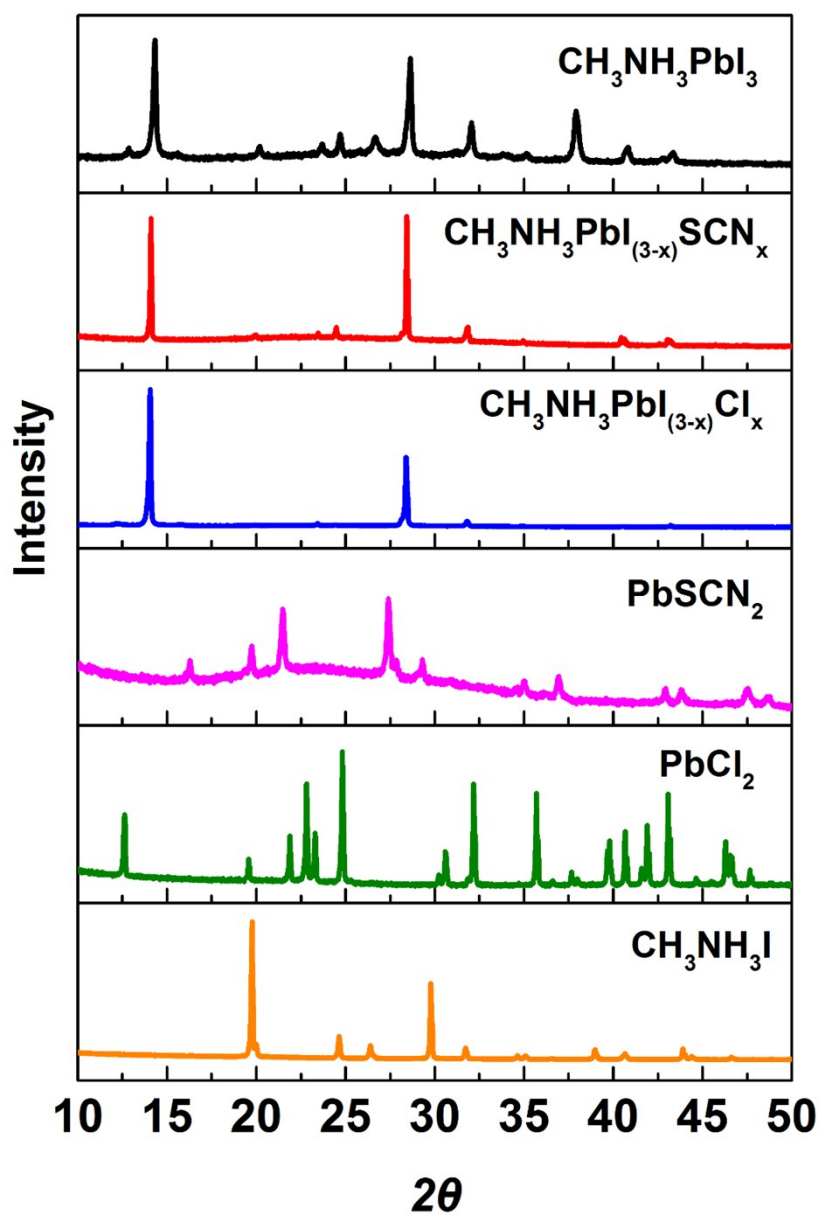


Fig.S12 XRD Spectra of the CH₃NH₃PbI_{3-x}(SCN)_x, CH₃NH₃PbI_{3-x}Cl_x, PbCl₂, Pb(SCN)₂ and CH₃NH₃PbI₃ Films and CH₃NH₃I powder.

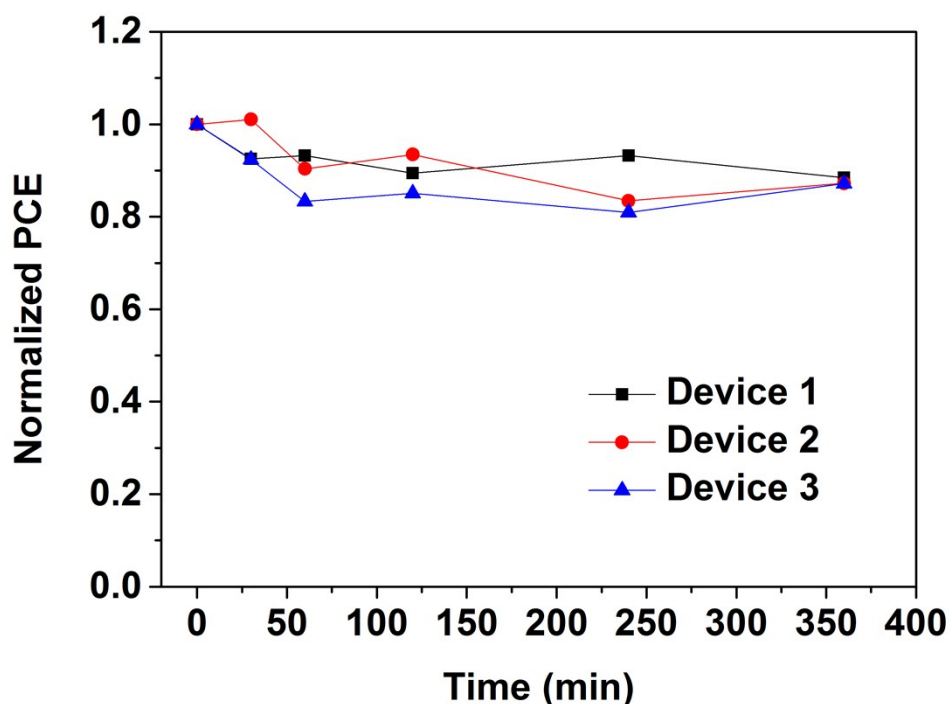


Fig.S13 Thermal stability studies (50 °C heated at ambient atmosphere) unsealed semitransparent devices (prepared from precursor solution $\text{Pb}(\text{SCN})_2 : \text{CH}_3\text{NH}_3\text{I}=1:3$)

We used the Digital Infrared Video Thermometer to test the temperature of the our unsealed semitransparent devices which has been exposed to simulated AM 1.5 sunlight under ambient environment for 1 hour and the test result showed that device working temperature is around 43.9°C. Therefore we heated our unsealed semitransparent devices to 50 °C at ambient atmosphere after a certain time and then test the PCE of device. The result showed that devices' PCE% had an average decrease of 12.4 % after heated for 360 min and we believe that further improvement can be achieve by using other method such as capsulation.

Reference

1. Bu, L.; Liu, Z.; Zhang, M.; Li, W.; Zhu, A.; Cai, F.; Zhao, Z.; Zhou, Y., Semitransparent Fully Air Processed Perovskite Solar Cells. *ACS Appl Mater Inter* **2015**, *7* (32).
2. Eperon, G. E.; Burlakov, V. M.; Goriely, A.; Snaith, H. J., Neutral color semitransparent microstructured perovskite solar cells. *ACS Nano* **2014**, *8* (1), 591-8.
3. Aharon, S.; Layani, M.; Cohen, B.-E.; Shukrun, E.; Magdassi, S.; Etgar, L., Self-Assembly of Perovskite for Fabrication of Semitransparent Perovskite Solar Cells. *Advanced Materials Interfaces*

2015, 2 (12), Article number:1500118.

4. Chang, C. Y.; Chang, Y. C.; Huang, W. K.; Lee, K. T.; Cho, A. C.; Hsu, C. C., Enhanced Performance and Stability of Semitransparent Perovskite Solar Cells Using Solution-Processed Thiol-Functionalized Cationic Surfactant as Cathode Buffer Layer. *Chem Mater* **2015**, *27* (20), 150926121850002.
5. Jin, H. H.; Han, H. J.; Lee, M.; Song, M.; Dong, H. K.; Sang, H. I., Stable semi-transparent CH₃NH₃PbI₃ planar sandwich solar cells. *Energ Environ Sci* **2015**, *8* (10), 2922-2927.
6. Roldán-carmona, C.; Malinkiewicz, O.; Betancur, R.; Longo, G.; Momblona, C.; Jaramillo, F.; Camacho, L.; Bolink, H. J., High efficiency single-junction semitransparent perovskite solar cells. *Energ Environ Sci* **2014**, *7* (9), 2968-2973.
7. Quiroz, C. O. R.; Levchuk, I.; Bronnbauer, C.; Salvador, M.; Forberich, K.; Huemüller, T.; Hou, Y.; Schweizer, P.; Spiecker, E.; Brabec, C. J., Pushing Efficiency Limits for Semitransparent Perovskite Solar Cells. *J Mater Chem A* **2015**, *3* (47), 24071-24081.
8. Eperon, G. E.; Bryant, D.; Troughton, J.; Stranks, S. D.; Johnston, M. B.; Watson, T.; Worsley, D. A.; Snaith, H. J., Efficient, Semitransparent Neutral-Colored Solar Cells Based on Microstructured Formamidinium Lead Trihalide Perovskite. *J Phys Chem Lett* **2015**, *6* (1), 129-138.
9. Gaspera, E. D.; Peng, Y.; Hou, Q.; Spiccia, L.; Bach, U.; Jasieniak, J. J.; Cheng, Y. B., Ultra-thin high efficiency semitransparent perovskite solar cells. *Nano Energy* **2015**, *13*, 249-257.
10. Guo, F.; Azimi, H.; Hou, Y.; Przybilla, T.; Hu, M.; Bronnbauer, C.; Langner, S.; Spiecker, E.; Forberich, K.; Brabec, C. J., High-performance semitransparent perovskite solar cells with solution-processed silver nanowires as top electrodes. *Nanoscale* **2015**, *7* (5), 1642-9.